Symmetric sampling

By GIJS J.O. VERMEER
Shell Research
Rijswijk, The Netherlands

In recent years, the seismic data acquisition technique has received renewed interest. In particular, Nigel Anstey (*Whatever happened to ground roll,* March 1986 *TLE*) and L. Ongkiehong and H. Askin (*Towards the universal seismic acquisition technique,* June 1988 *First Break*) introduced new ideas. These authors argue that ground roll suppression is optimal if the acquisition technique insures a regular distribution of geophones over the common midpoint.

Using real data examples, P.F. Morse and G.F. Hildebrandt (*Ground roll suppression by the stack-array,* GEOPHYSICS 1989) and M.A. Ak (*How effective is the stack array?* presented at the 1990 EAEG meeting in Copenhagen) demonstrated the superior performance of the stack-array approach over techniques in which there is no such regular distribution of geophones.

In my book *Seismic Wavefield Sampling* (published by SEG in 1990), I expand the idea of regularity to the sampling of both receivers and shots. This paper deals with some highlights of that book, concentrating on the concept of symmetric sampling as the best compromise data acquisition technique.

The shot/receiver- and midpoint/offset coordinate systems. This section introduces the terminology and describes some basics of the prestack seismic data set for a 2-D line.

In the field, the prestack data are gathered in subsets called common shot gathers, one at a time. Taken together, the common shot gathers form a 3-D data set, which is smooth and continuous (apart from shot and geophone coupling variations).

There are three independent coordinates: traveltime (t), and two spatial coordinates—midpoint (x_m) and offset (x_o). The same data can also be described by traveltime (t), source coordinate (x_s) and receiver coordinate (x_r). These symbols are illustrated in Figure 1. The two pairs of spatial coordinates are related by:

$$x_m = (x_s + x_r)/2 \qquad x_s = x_m + x_o/2$$

and

$$x_o = x_s - x_r \qquad x_r = x_m - x_o/2$$

A description of a prestack seismic data set in the two coordinate systems is shown in Figures 2a and 2b. In Figure 2a, the data set is described in terms of shot and receiver coordinates. This surface diagram was introduced by Turhan Taner et al. in *Estimation and correction of near-surface time anomalies* (August 1974 GEOPHYSICS), to describe static correction procedures. Figure 2b describes the same prestack data set in the midpoint/offset coordinate system. This representation is also called the subsurface diagram or stacking diagram.

By keeping one of the spatial coordinates constant, four different subsets can be selected from the seismic data set. These subsets are indicated in Figures 2a and 2b. Note that all traces of a common shot gather with x_s = constant are represented by a horizontal line in the shot/receiver coordinate system and by an oblique line in the midpoint/offset coordinate system.

By keeping the time coordinate constant, a time slice is generated from the prestack seismic data set. In a time slice, the spatial coordinates vary so that the surface and subsurface diagrams could also be regarded as a description of the data points in a time slice.

We are inclined to think of reflections in prestack data as hyperbolas in the common midpoints. However, it is important to realize that each event represents a surface in the 3-D space of the prestack seismic data set. The three dimensions of the prestack data should not be confused with the three dimensions of the subsurface. In prestack data, offset is the third dimension. Take, for example, a dipping event as shown in Figure 3 which reveals the three orthogonal cross sections: common midpoint, common offset, and common time. The shape of a dipping event is a hyperbola in the common midpoint and an ellipse in the time slice.

A real data example is given in Figure 4. Of course, now there is a multitude of events, all having their own spatial and temporal relationships. Actually, the common offset panel in this example is a stack which is basically a zero-offset section with a relatively high signal-to-noise ratio. It is possible to follow dipping events through all three cross sections.

Creating time slices from the prestack data of a 2-D line can be a very rewarding exercise. Time slices increase insight in the characteristics of the data and allow useful diagnostics-at-a-glance

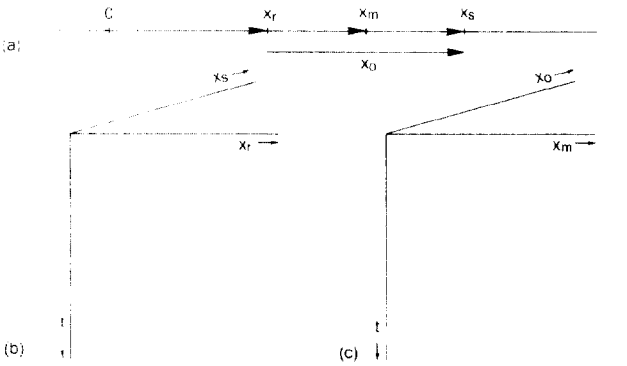

Figure 1. Prestack data coordinate systems. (a) The four spatial coordinates in relation to the seismic line. (b) Shot/receiver coordinate system. (c) Midpoint/offset coordinate system.

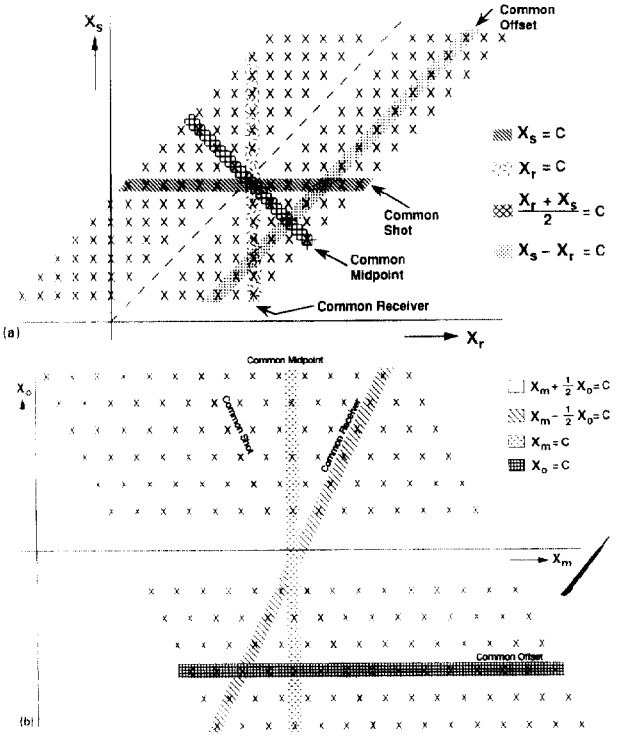

Figure 2. Descriptions of prestack seismic data set in (a) shot/receiver coordinate systems and (b) midpoint/offset coordinate systems. The former is also called a surface diagram and the latter a subsurface diagram or stacking diagram.

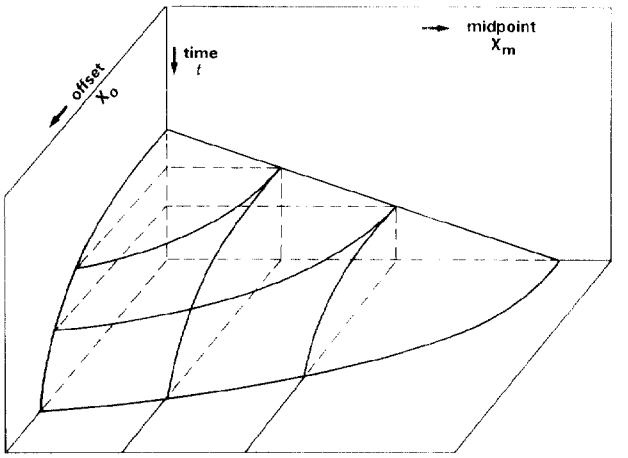

Figure 3. Dipping event in midpoint/offset coordinate systems. The event is a hyperbola in the common offset panels (a straight line for zero offset), a hyperbola in the CMP, and an ellipse in the time slice.

of the whole data set. Time slices created after NMO correction allow a quick quality control of the chosen velocities for the level of interest.

For proper sampling of the temporal coordinate, it is important to know the maximum frequency of the data to be sampled. Likewise, for spatial sampling, the maximum wavenumber of the spatial coordinates must be known. A discussion of spatial sampling requires the introduction of four different wavenumbers (k_s, k_r, k_m, k_o) corresponding to the four spatial coordinates (x_s, x_r, x_m, x_o). Similar to the pairs of spatial coordinates (x_s,x_r) and (x_m, x_o), there is also a linear relationship between the pairs of wavenumbers:

$$k_m = k_s + k_r \qquad k_s = k_m/2 + k_o$$

and

$$k_o = (k_s - k_r)/2 \qquad k_r = k_m/2 - k_o$$

It is possible to compute *f-k* spectra for common shot panels, common receiver panels, common midpoint panels, and common offset panels. Or, the double wavenumber spectrum of a time slice can be computed. One may also think of computing the double wavenumber spectrum of a common frequency panel.

Whatever subset is considered, it is important to distinguish the various ks from each other because they represent very different physical effects. In particular, the offset wavenumber (k_o) describes velocity effects in the common midpoint panel, and the midpoint wavenumber (k_m) describes structure effects in the common offset panel. For instance, for a horizontal earth, there are only horizontal events in the common offset panel. So the wavenumber spectrum of that panel only shows energy at k_m = 0. In more practical cases, there is also energy for larger midpoint wavenumbers.

Symmetric sampling. The data I have described in the surface and subsurface diagrams (Figures 2a and 2b) have already been sampled. Figure 5 shows the spatial sampling interval used for the surface diagram. In this case, the shot interval is the same as the receiver (or group) interval.

Now we have to ask ourselves the all-important question: What is the best way of sampling these two spatial coordinates?

To answer this question, we must know the properties of the 3-D wavefield to be sampled. As shot and receiver coordinates are sampled independently, the properties of the wavefield, both in the common shot gather and in the common receiver gather, need to be examined.

The common shot gather is the result of a physical experiment; therefore, the properties of the wavefield of the common shot gather are described by elastic wave theory. On the other hand, the traces of a common receiver gather are all recorded separately at different times with different shots. So what are the properties of the wavefield in the common receiver gather? Here we will use reciprocity. It follows from the principle of reciprocity that the common receiver gather recorded by a receiver at p is in its entirety identical to the common shot gather for which the shot is located at p (see Figure 6). Hence, the properties of the wavefield in the common receiver gather are the same as in the common shot gather and, as a consequence, sampling of shot coordinate and receiver coordinate has to be the same.

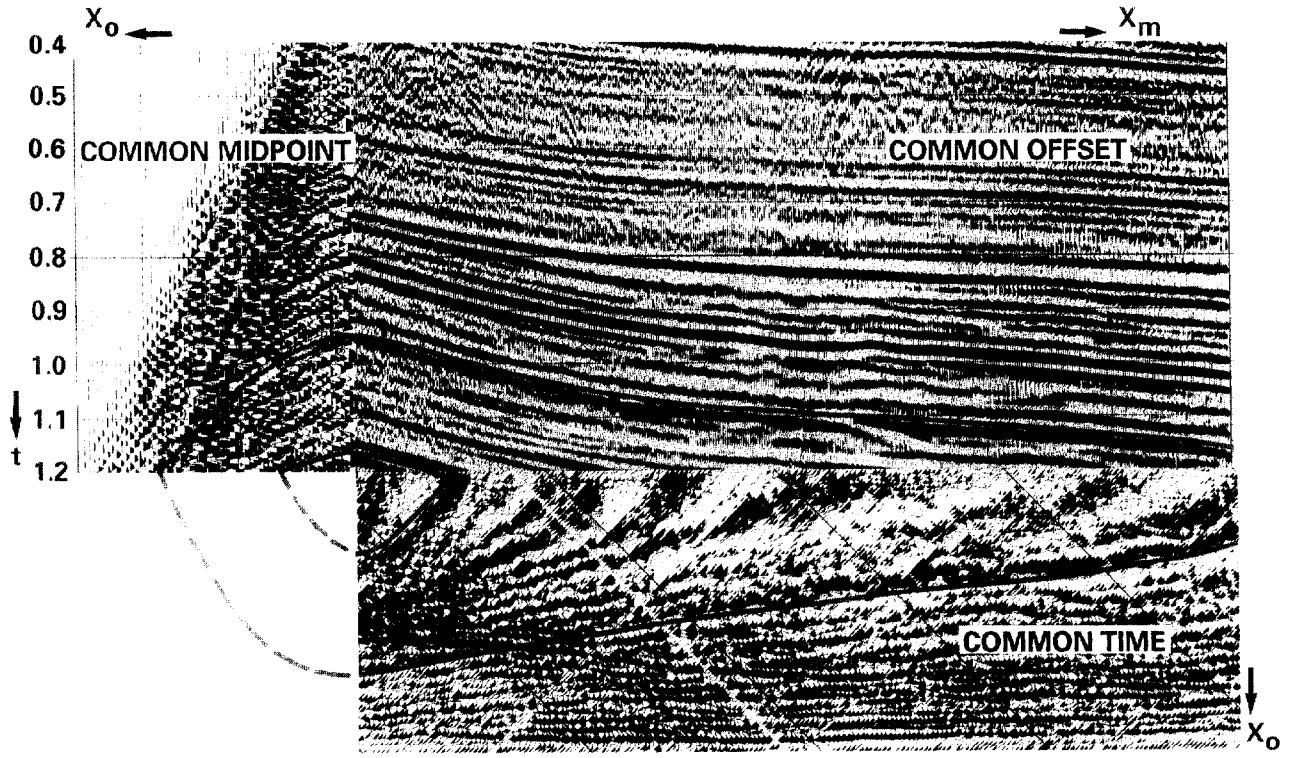

Figure 4. Three cross sections through real prestack data set. Note that each event is a surface in 3-D t, x_m, x_o space.

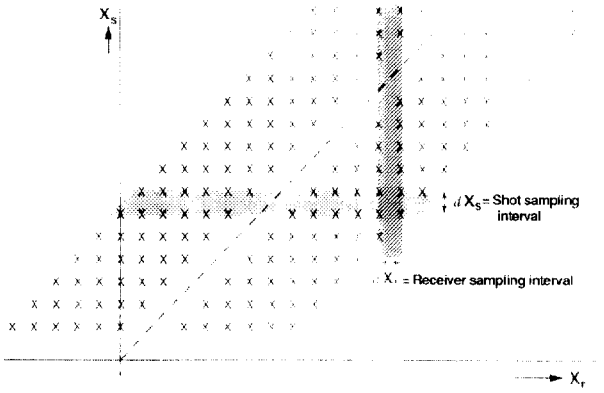

Figure 5. Shot and receiver sampling intervals in the surface diagram.

We would like to record the two spatial coordinates without aliasing, just as we do with the temporal coordinate. Figure 7 illustrates that the maximum wavenumbers $|k_s|_{max}$ and $|k_r|_{max}$ are determined by the maximum frequency, f_{max}, of the event with the slowest apparent phase velocity, V_{min}. In three-dimensional (f, k_s, k_r) space, the energy of the wavefield is confined to a pyramid-shaped volume with its base at $f = f_{max}$ (Figure 8). Alias-free spatial sampling is achieved if the maximum wavenumbers are properly sampled, which means that neither shot interval nor receiver interval should be larger than $1/2k_{max}$. Or, in other words, these intervals should not be larger than a half-period of the smallest wavelength.

The requirement of alias-free spatial sampling leads to spatial sampling intervals that are much smaller than considered practical or affordable (e.g., for f_{max} = 75 Hz, V_{min} = 300 m/s, the shot and receiver intervals should be 0.5*300/75 = 2 m). As a compromise, seismic field arrays are to be used which act as spatial antialias filters and as resampling operators. As spatial antialias filters, they aim to attenuate all energy above the Nyquist wavenumber. Spatial antialias filtering must be applied when sampling both spatial coordinates. In other words, shot arrays are as necessary as receiver arrays and, for optimal results, shot arrays should be identical to receiver arrays. This reasoning leads to the concept of symmetric sampling:

- Shot interval equal to receiver interval
- Shot arrays equal to receiver arrays

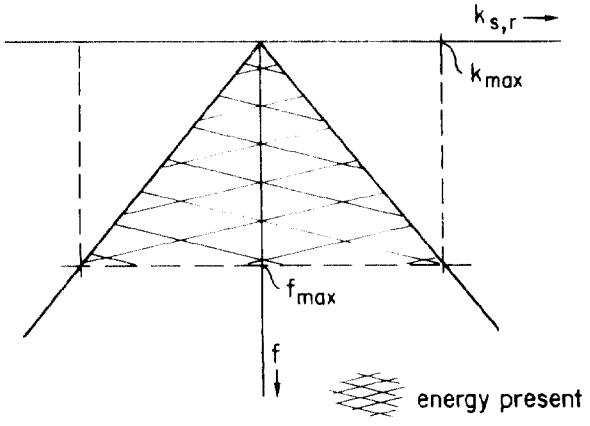

Figure 7. Regions with and without energy in f, k_s and f, k_r. Maximum frequency of event with minimum phase velocity determines maximum wavenumber and it is the same for shot and receiver coordinate.

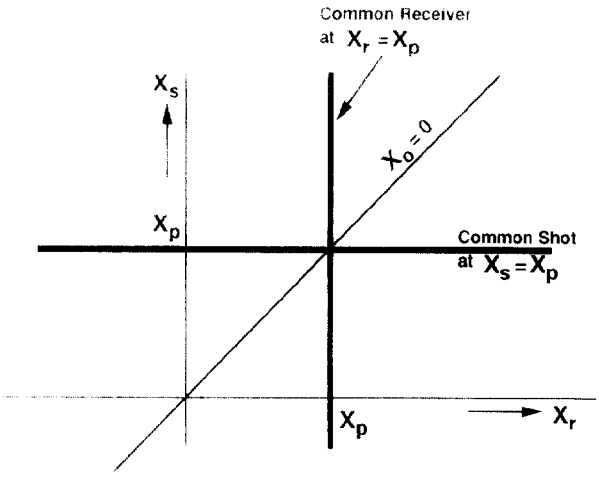

Figure 6. Common shot gather at $x_s = x_p$ and common receiver gather at $x_r = x_p$ are identical because of reciprocity.

I call this technique symmetric sampling because it utilizes the symmetry property of reciprocity and it preserves the inherent symmetry of the prestack wavefield.

Figures 9a,b,c illustrate the concept. (In these figures the x_s, x_r coordinate system has been rotated 45° for ease of display.) To keep the pictures simple, I used only three elements per array (when there is an array). Figure 9a shows an asymmetric configuration with no shot array and three geophones per geophone array. Each recorded trace is the sum of three elemental traces registered by the three geophones of the geophone array. The groups of three elemental traces are represented by alternating between three open circles and three closed circles. Note that the three elemental traces for a given recorded trace have different offsets and different midpoint positions. Summing these elemental traces causes some damage to the signal, but this is the price to be paid for the antialias effect of the geophone array. In Figure 9b, a symmetric sampling configuration is shown. Now there is also a shot array consisting of three elements so that each recorded trace corresponds to nine elemental traces. Note that, again, each of the elemental traces occupies a different position in the shot/receiver coordinate system. Together, all the elemental traces provide a regular two-dimensional sampling of the shot/receiver plane. Compare this with Figure 9a, where whole areas of the plane are not sampled. These empty areas may lead to spatial alias-

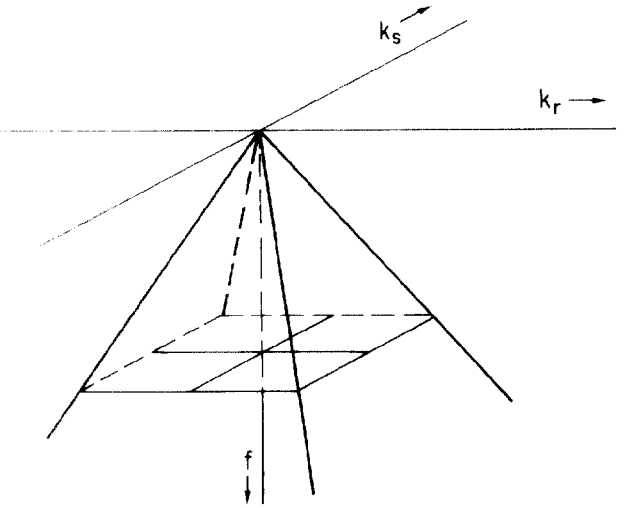

Figure 8. Energy of prestack data wavefield is confined to pyramid shaped volume in f, k_s, k_r. Base of pyramid is at $f = f_{max}$.

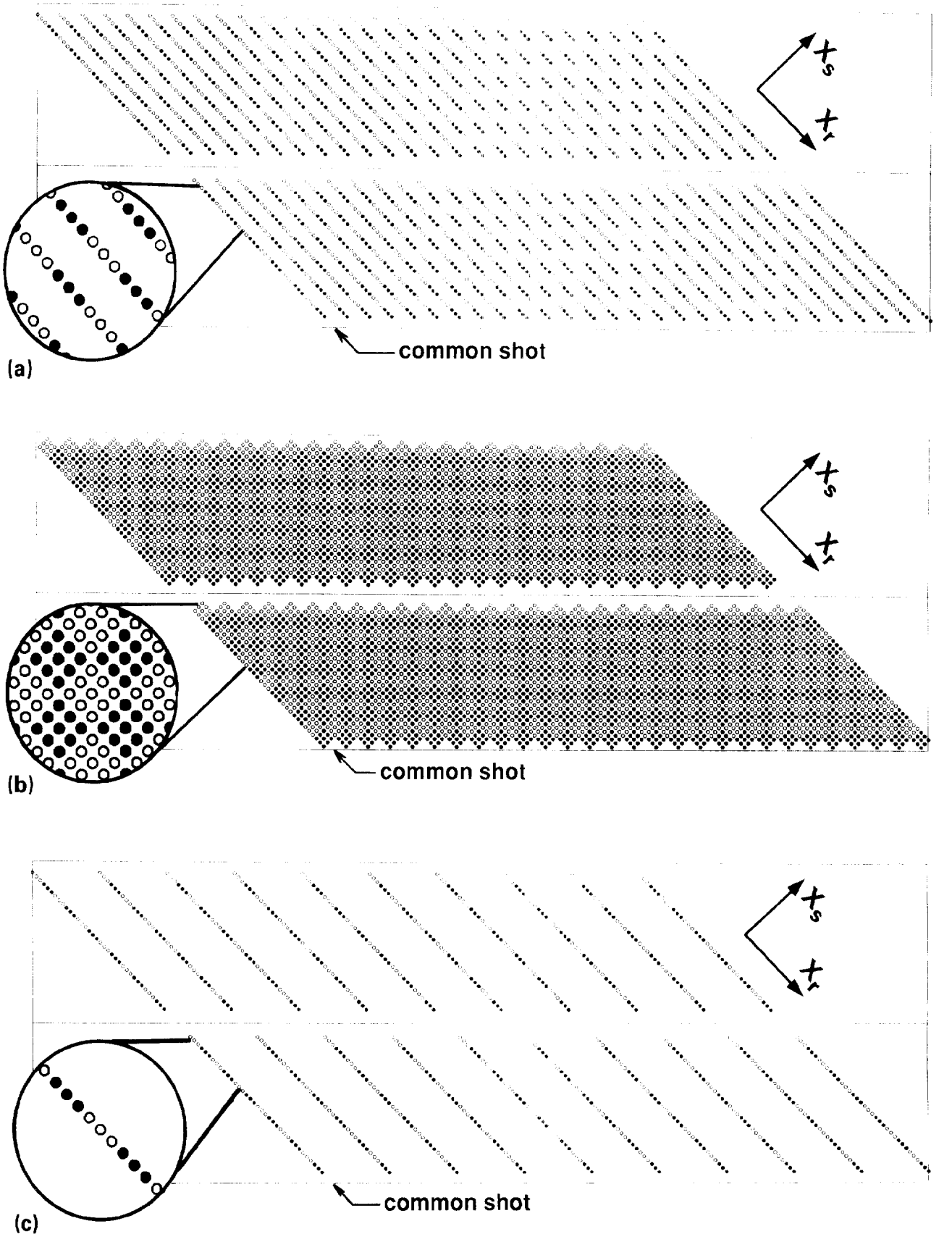

Figure 9. Various center-spread shooting geometries with three elements per array, when there is an array. Each symbol represents an elemental shot/receiver pair; each group of equal symbols (either open circles or closed circles) represents one recorded trace. (a) Asymmetric configuration with shot interval equal to receiver station interval, and a geophone array but no shot array. (b) Symmetric configuration with shot interval equal to receiver station interval, and both geophone and shot arrays. (c) Asymmetric configuration with shot interval three times receiver station interval. Note the large unsampled area of shot/receiver space.

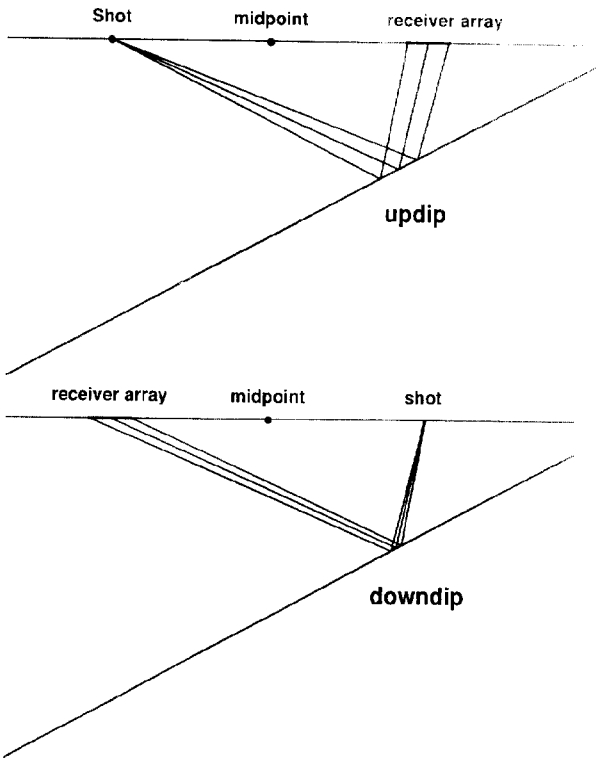

Figure 10. Updip versus downdip shooting for an asymmetric configuration with a geophone array but no shot array.

ing in the common receiver domain and also in the common midpoint and common offset domains.

Another, perhaps even more common, example of asymmetric sampling is shown in Figure 9c. Now the shot interval is three times the group interval. Here even more of the shot/receiver plane is not sampled.

Whether or not spatial aliasing occurs for a particular shooting geometry (symmetric or asymmetric) and how large the effect is depends on the distance between the array elements and on the shot and receiver intervals. Symmetrically sampled data may still be aliased if the sampling intervals are too large, and asymmetrically sampled data may not show aliasing if the sampling intervals are small enough (see, also, final paragraph of next section)

Some effects of asymmetric sampling. These effects are different for off-end shooting and center-spread shooting. For the former, asymmetric sampling leads to differences between updip and downdip shooting. Figure 10 illustrates that for updip shooting, there is less of a difference between the arrival times of the reflections over the length of the receiver array than there is for downdip shooting. As a consequence, the reflection character is less affected by updip shooting than by downdip shooting. Asymmetric sampling also leads to asymmetries on either side of the apex of diffractions.

Asymmetric sampling is more or less the norm in marine data acquisition, as shot layouts are usually not designed to be similar to receiver arrays. The asymmetric shooting geometry affects left- and right-dipping events in a different way, leading to differences in parallel lines shot in opposite directions. This effect also causes jitter in the crossline direction of marine 3-D surveys.

In center-spread recording, the effect of asymmetric sampling is less visible in the stack, as the asymmetry of the sampling is hidden by the symmetry of the spread. However, the differences between up-dip and down-dip shooting, as discussed for off-end recording, now occur in the recording of one and the same line. Now the effect becomes visible in the common midpoint gathers as an odd-even or checkerboard effect. I have simulated the effect in the example shown in Figures 11a,b. Figure 11a is a CMP with equal shot and receiver arrays, whereas in Figure 11b the receiver

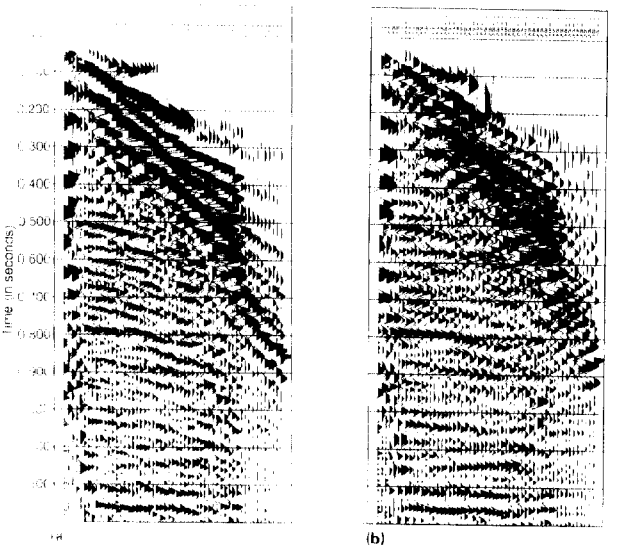

Figure 11. Symmetric versus asymmetric sampling in center-spread geometry. Shot interval equals receiver interval. CMPs are displayed with increasing absolute offset (i.e., neighboring traces originate from different ends of the spread). (a) Symmetric data, shot array = receiver array = 25 m. (b) Asymmetric data, shot array = 25 m, receiver array = 75 m. Note the odd/even effect in the asymmetrically sampled CMP.

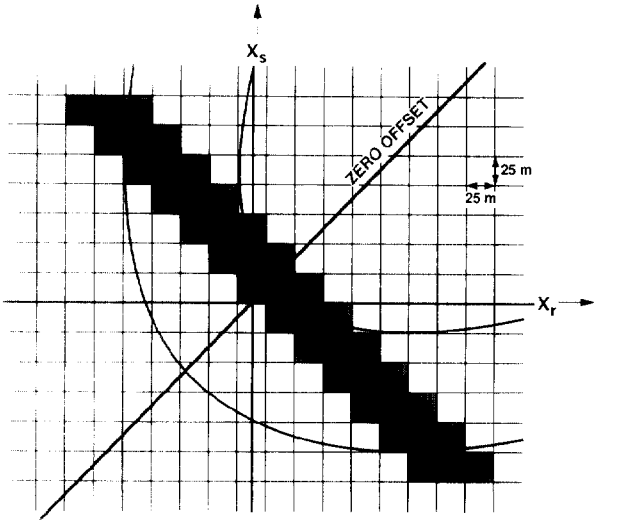

Figure 12. Explanation of odd/even effect in CMP of asymmetrically sampled data. Curved lines represent constant time lines of a dipping event (compare with Figure 3). Each rectangle is the convolution of a short 25 m shot array with a long 75 m geophone array. The elemental traces within a rectangle are added to form one recorded trace in the CMP. In the top left corner, the addition takes place across the time lines of the dipping event, whereas in the bottom right corner, the addition is mostly parallel to the time lines.

arrays are three times as long as the shot arrays (75 m versus 25 m). I constructed the right panel using a three-trace running mix in the common shot panels, followed by CMP sort. In both CMPs, the traces are sorted according to increasing absolute offset. The right panel now shows an odd-even jitter. The jitter occurs for events that dip in the common offset panel. The explanation of the odd/even jitter follows from the difference in averaging effects of the arrays on either side of zero offset.

This averaging effect is illustrated in Figure 12 in which the two curved lines represent constant time lines of a dipping event in the shot/receiver plane. (As discussed earlier, these lines are ellipses.) The lines are symmetric with respect to the diagonal

which is the zero-offset line. The rectangles represent traces of one common midpoint with each trace formed by a 25 m shot array and a 75 m receiver array. In the top left corner, the rectangle averages across the time lines; in the lower right corner, the rectangles run more or less parallel to the time lines. This difference in averaging leads to a different character between positive and negative offsets. Similar odd/even effects can be observed with single hole dynamite shooting. I am sure many seismic processors have noticed those effects. Obviously, it leads to a suboptimal stack for center-spread recording.

The severity of asymmetric sampling depends on a number of factors, such as spatial sampling intervals, degree of asymmetry, relative strength of coherent noise, dip (stronger dip, larger effects), and geologic complexity. With some further analysis, some of those effects may be quantified (for instance, the increasing severity with increasing dip).

On the other hand, symmetric sampling has numerous advantages:

- Symmetry of wavefield is preserved
- Character independent of line direction (off-end shooting)
- Constant character across CMP (center-spread shooting)
- Better coherent noise suppression
- Data better suited for cascaded shot- and receiver-domain processing
- Data better suited for highly sophisticated processes such as AVO analysis, migration, inversion

These advantages, in turn, lead to fewer and less severe low quality data zones, better resolution of complex geology, and better porefill and lithology prediction; in short, a more reliable and successful interpretation. Whether or not these advantages materialize depends, to a large extent, on the ability to even out variations in shot strength and geophone coupling with surface-consistent equalization.

I would like to point out that symmetric sampling with large sampling intervals is likely worse than asymmetric sampling with smaller sampling intervals. It is important to use sufficiently small spatial sampling intervals. A nice compromise to aim for is to use shot and receiver intervals that would record the desired wavefield without aliasing up to the frequency of interest. Then arrays are only necessary to suppress noise and to average out sampling irregularities. This technique is called full-resolution recording.

The stack-array approach versus symmetric sampling. Briefly, the difference is that Anstey emphasizes a regular sampling of geophones (across the CMP), whereas symmetric sampling calls for regular sampling not only of geophones but also of shots. The stack-array approach does not specify the use of shot arrays, leading to an asymmetric sampling technique (as shown in Figure 9a). The common shot gather is properly sampled, but aliasing may occur in the common receiver gathers. Nevertheless, I want to stress that Anstey's technique is a tremendous improvement over older techniques using large shot intervals (such as illustrated in Figure 9c).

The total stack response. Finally, it is of great interest to investigate the combined response of field arrays and stacking which can be called the total stack response. This can be written as the product of three individual responses—the shot array response, the receiver array response, and the so-called CMP-array response, or:

$$S(k_m, k_o) = p(k_s) \times p(k_r) \times p(k_m) .$$

The three responses involve three different wavenumbers. For uniform arrays with element spacing d and number of elements N, the array response is

$$p(k) = \sin(N\pi kd) / N \sin(\pi kd) ,$$

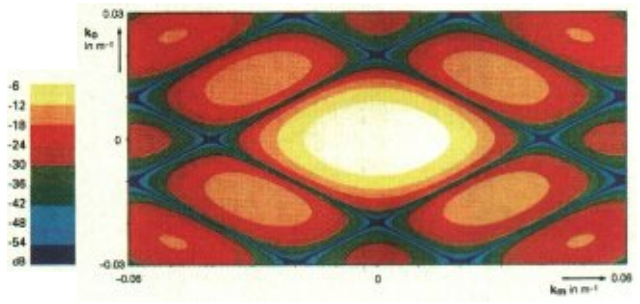

Figure 13. Combined response of shot and receiver arrays in midpoint/offset wavenumber domain. Oblique dark blue lines represent notches in the shot array and receiver array responses.

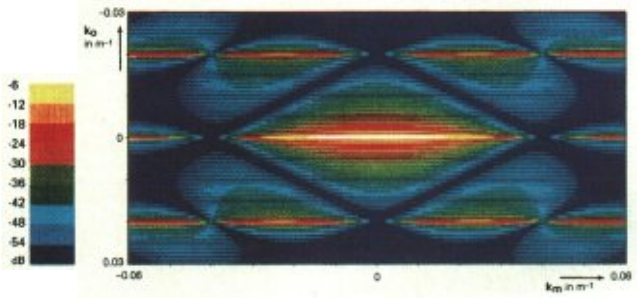

Figure 14. Total stack response for a symmetric sampling technique. The notches of the CMP array run parallel to the k_m axis.

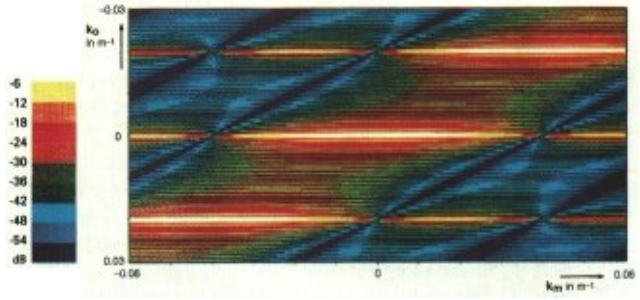

Figure 15. Total stack response for an asymmetric sampling technique without a shot array. Note the greatly reduced suppression and the asymmetry in the response.

so that the first notch of this array occurs at $k = 1/Nd$. Nd is called the array length, and not $(N-1)*d$. In the examples, I will use 50 m field arrays and 1200 m offset range, hence the first notches of the three arrays occur at $k_s = 1/50$, $k_r = 1/50$, and $k_o = 1/1200$ m^{-1}. (This discussion does not take NMO into account; see previously cited articles for the effect of NMO on the array responses.)

Using the linear relationships between the wavenumber pairs, the total stack response can be written as a function of only two wavenumbers. Figure 13 shows the product of only the responses of a 50 m shot array and a 50 m receiver array in the midpoint-offset wavenumber domain. Lines of constant shot and receiver wavenumber run obliquely in this domain. Note the diamond-shaped passband of the two arrays in the 2-D wavenumber domain.

A common mistake is to compute the product of the two array responses as a function of only one wavenumber. This product describes the effect of the arrays on a horizontal earth with no midpoint dependence. The horizontal earth response is found along the vertical axis of Figure 13. However, any dipping events will contain energy away from the vertical axis and will be affected differently by the field arrays. So, the correct representation uses the double wavenumber domain. As a bonus, this procedure also creates pictures that are pleasing to the eye.

Figure 14 shows the total stack response for a symmetric sam-

pling technique with center-spread recording and an offset range −1200 to 1200 m. Note that the stack produces notches parallel to the horizontal k_m axis. The diamond-shaped passband of the field arrays has now been reduced to a narrow passband centered around the midpoint wavenumber axis. Everywhere else the combination of field patterns and stack is supposed to suppress all energy. As is clear from the picture, the suppression is certainly not uniform although it is symmetric. There are areas of very good suppression where all three arrays are effective, and there are also areas of less good suppression. (The parameters of this example should not be taken as recommended symmetric sampling field parameters; usually, considerably smaller intervals are necessary for good results.)

How much unwanted energy is left after application of the three arrays depends on:

- Energy distribution of the prestack wavefield
- Choice of field parameters (shot and receiver interval, and multiplicity)
- Choice of pre- and poststack processing parameters

Leaving out the shot array has a dramatic effect on the total stack response (as shown in Figure 15). The severity of not using a shot array or any other form of asymmetric sampling depends on the energy distribution of the original continuous wavefield in the (k_m,k_o)– wavenumber domain. If there are many rapid variations as a function of midpoint, then asymmetric sampling will do more harm than if the geology varied more slowly.

Finer sampling (shorter shot and receiver arrays) pushes the filter notches out toward larger wavenumbers. As a consequence, a larger part of the original wavefield will fall in the passband of the combined field arrays. In the passband, more of the suppression of the unwanted events is then left to the stack and to other digital processes. Digital processes such as *f-k* filtering in the common midpoint and common offset panels are usually required to compensate for the reduced effect of the two field arrays.

Conclusions. Symmetric sampling is the preferred recording technique, so it should be high on the "wish list" of every interpreter.

The parameters of symmetric sampling are a compromise and they need to be established after an evaluation of the geologic and geophysical problems at hand.

A better understanding and knowledge of the energy distribution in f, k_m, k_o would help predict the effect of any choice of the acquisition parameters. Noise spreads and very densely sampled multiple-coverage data can be used to help gain such insights.

As a final comment, I would like to remind the reader of the fact that we are going to very great lengths to apply the most sophisticated processing techniques—inversion and AVO in particular. These efforts are bound to be futile if they are applied to data recorded in a suboptimal way. LE

Acknowledgments: I am indebted to Jeff Deere for his conscientious review of this paper. I'd like to thank Shell Internationale Petroleum Maatschappij and Shell Research B.V. for their permission to publish this article.

Gijs Vermeer received an MSc in mathematics from the Technological University of Delft in 1965. After military service he joined Shell Research where he carried out seismic processing research, followed by eight years in Shell Expro (London) and NAM (The Netherlands). Vermeer joined Shell Canada in 1988 where he was involved in stratigraphic interpretation of carbonate reefs. Recently he moved back to Shell Research in The Netherlands, this time to work on seismic data acquisition. Vermeer is a member of SEG, EAEG, and CSEG.